

Simultaneous Jahn-Teller distortion and magnetic order in the double perovskite $\text{Ba}_2^{154}\text{SmMoO}_6$

A. C. McLaughlin*

Department of Chemistry, University of Aberdeen, Meston Walk, Aberdeen AB24 3UE, United Kingdom

(Received 21 December 2007; revised manuscript received 11 September 2008; published 6 October 2008)

An unexpectedly high antiferromagnetic transition temperature ($T_N=130$ K) has been observed in the double perovskite $\text{Ba}_2^{154}\text{SmMoO}_6$ as a result of a strong interplay between spin, orbital, and lattice degrees of freedom. The crystal structure distorts from tetragonal (space group $I4/m$) to triclinic (space group $I-1$) as the temperature is reduced below 353 K. A Jahn-Teller distortion is observed at T_N so that a tetragonal elongation of the MoO_6 octahedra is observed. It is suggested that orbital order precipitates antiferromagnetic order with anomalously high T_N in the $4d^1$ Mo^{5+} $\text{Ba}_2\text{REMoO}_6$ (RE=Sm, Eu) double perovskites.

DOI: [10.1103/PhysRevB.78.132404](https://doi.org/10.1103/PhysRevB.78.132404)

PACS number(s): 75.50.Ee, 71.70.Ej, 75.30.Et

diffraction study has been performed on $\text{Ba}_2^{154}\text{SmMoO}_6$ between 4 and 353 K.**I. INTRODUCTION**

Exotic electronic, magnetic, and structural phenomena have been observed in doped transition-metal oxides in recent years; one such example is colossal magnetoresistance (CMR). CMR materials undergo a large reduction in the electrical resistance upon application of a magnetic field and are used in spintronic devices. CMR is established in perovskite manganites such as $\text{La}_{1-x}\text{Sr}_x\text{MnO}_3$ for Mn oxidation states of 3.2–3.5.¹ LaMnO_3 , the parent compound to the CMR manganites, contains the Jahn-Teller active Mn^{3+} ion and a strong interplay between spin, orbital, and structural degrees of freedom is observed as the cooperative Jahn-Teller distortion is accompanied by *C*-type orbital ordering and *A*-type antiferromagnetism. A coupling between spin, orbital, and lattice degrees of freedom has also recently been observed in other $3d$ transition-metal compounds such as Sr_2VO_4 (Ref. 2) and KCrF_3 .³ The cooperative Jahn-Teller distortion observed in the latter material is accompanied by orbital ordering and weak ferromagnetism which is reminiscent of what is observed in LaMnO_3 , the parent compound of the CMR manganites.

In contrast to the examples above in which orbital order of the e_g states occurs, the observation of a cooperative Jahn-Teller distortion in materials with unevenly filled t_{2g} orbitals is much less common. Most recently ferromagnetism has been observed at low temperature in the Mott insulator $\text{Ba}_2\text{NaOsO}_6$ (Ref. 4) as a result of orbital ordering where Os^{7+} has the $5d^1$ electronic configuration. We have previously studied the magnetic and electronic properties of the Mo based oxides, $\text{Ba}_2\text{REMoO}_6$ (RE=Sm, Eu, Gd, Dy),⁵ in which Mo is pentavalent and has the electronic configuration t_{2g}^1 which is sensitive to a Jahn-Teller instability. These materials were originally synthesized by Brandle and Steinfink⁶ but the magnetic and electronic properties had not been studied. All samples were found to be electronically insulating. Antiferromagnetic order was observed from dc susceptibility measurements on $\text{Ba}_2\text{SmMoO}_6$ and $\text{Ba}_2\text{EuMoO}_6$ with anomalously high T_N of 130 and 112 K, respectively.^{5,7} There was no evidence of magnetic order for $\text{Ba}_2\text{REMoO}_6$ (RE=Gd-Yb, Y).^{5,7,8} Previous studies had demonstrated antiferromagnetic order at 15 K in $\text{Ba}_2\text{NdMoO}_6$ (Ref. 7) and 4 K in $\text{Sr}_2\text{ErMoO}_6$.⁹ In order to further investigate the anomalously high T_N observed for $\text{Ba}_2\text{SmMoO}_6$ and $\text{Ba}_2\text{EuMoO}_6$ and to see if there is a correlation between T_N and orbital order of the t_{2g} states a variable-temperature neutron-

II. EXPERIMENT

^{150}Sm has a high absorption cross section for thermal neutrons and hence samples were synthesized with the less absorbing ^{154}Sm isotope. $\text{Ba}_2^{154}\text{SmMoO}_6$ was prepared by the solid-state reaction of stoichiometric oxides of $^{154}\text{Sm}_2\text{O}_3$, MoO_3 , and BaCO_3 powders. These were ground, die pressed into a pellet, and heated to 800 °C under flowing 5% H_2/N_2 and held at this temperature for 15 min. The temperature was then raised in intervals of 200 °C up to 1200 °C; the samples were held for 15 min at 1000 °C. Finally the pellets were annealed at 1200 °C for 4 h and then furnace cooled to ambient temperature. This step was repeated three times in order to ensure phase homogeneity.

Neutron-diffraction patterns were recorded at a wavelength of 1.5943 Å on instrument SuperD2B at the ILL, Grenoble. A 1 g sample was inserted into an 8 mm vanadium can and neutron-diffraction patterns were recorded with an acquisition time of 1 h at several temperatures between 5 and 353 K. Some weak impurity peaks were detected in the neutron-diffraction patterns but they were not intense enough to index and fit.

III. RESULTS AND DISCUSSION

The magnetization of $\text{Ba}_2^{154}\text{SmMoO}_6$ was recorded between 10 and 260 K on a Quantum Design superconducting quantum interference device (SQUID) magnetometer in an applied field of 1000 Oe after zero-field cooling (ZFC) and field cooling (FC) and an antiferromagnetic transition is evidenced at 130 K (Fig. 1). There is no significant deviation between FC and ZFC susceptibility data so that there is no evidence of weak ferromagnetism. Furthermore there is no evidence of hysteresis upon recording susceptibility data at 5 K between ± 1 T. An increase in the susceptibility is observed at low temperature which corresponds to the paramagnetic tail of unordered spins. The neutron-diffraction patterns were all fitted by the Rietveld method¹⁰ using the GSAS program.¹¹ The backgrounds were fitted using linear interpolation and the peak shapes were modeled using a pseudo-Voigt function. An excellent fit to the tetragonal space group $I4/m$ (tilt system $a^0a^0c^-$) is observed at 353 K

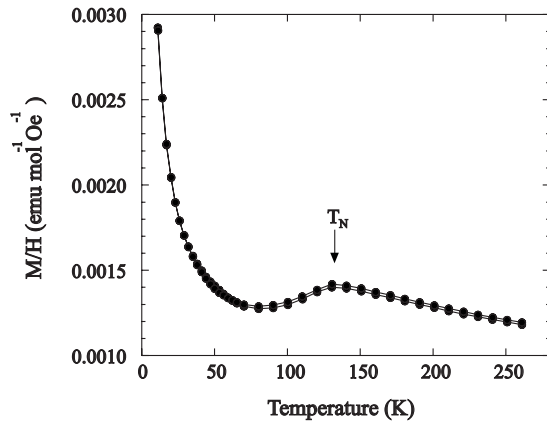


FIG. 1. Temperature dependence of the FC and ZFC magnetic susceptibilities for $\text{Ba}_2^{154}\text{SmMoO}_6$ recorded in a field of 1000 Oe; T_N is labeled.

[$a=6.0000(3)$ Å, $c=8.4919(7)$ Å, $\chi^2=2.25$, $R_{\text{WP}}=3.27\%$]. Below 353 K peak broadening of the high angle diffraction peaks suggested a structural distortion to a lower symmetry (Fig. 2). An excellent Rietveld fit to the triclinic $I-1$ space group [$a=5.9885(6)$ Å, $b=5.9910(6)$ Å, $c=8.5027(2)$ Å, $\alpha=89.95(1)$, $\beta=90.06(1)$, $\gamma=89.97(1)$, $\chi^2=3.86$, $R_{\text{WP}}=4.78\%$ ($a^-b^-c^-$)] was obtained at all temperatures below 353 K (Figs. 2 and 3). The same distortion is observed in $\text{Ba}_2\text{NdMoO}_6$ at low temperature.⁷ A group theoretical analysis¹² has previously demonstrated that additional octahedral tilting of the $I4/m$ structure results in distortion to the triclinic space group $I-1$ or to the monoclinic space group $C2/c$ ($a^0b^+c^-$). An attempt to model the data with monoclinic symmetry such as $C2/c$ resulted in an inferior fit to the data ($\chi^2=6.16$, $R_{\text{WP}}=6.2\%$). The data were also modeled with the monoclinic space group $I2/m$ ($a^0b^-b^-$), which has the same reflection conditions as $I-1$, but an inferior fit was also obtained ($\chi^2=5.42$, $R_{\text{WP}}=5.5\%$). The room-temperature x-ray diffraction pattern for $\text{Ba}_2\text{SmMoO}_6$ was previously indexed on the tetragonal space group $I4/mmm$.⁷ The neutron-diffraction results clearly show that at room-temperature triclinic symmetry is observed and that a transition to tetragonal $I4/m$ is observed at 353 K. The same space group is observed above the tetragonal to triclinic transition at much lower temperature in $\text{Ba}_2\text{NdMoO}_6$.⁷ There is no evidence of antisite disorder and the Mo^{5+} and Sm^{3+} site occupancies refine to 0.98(1) and 0.97(1), respectively. Refinement results are deposited in Ref. 13.

The reduction in symmetry from tetragonal to triclinic results in a distortion of the MoO_6 octahedra so that there are four long and two short Mo-O bonds [at 260 K Mo-O(1) (apical)=1.994(4) Å, Mo-O(2) (in plane)=1.965(10) Å, and Mo-O(3) (in-plane)=1.998(10) Å; at 353 K Mo-O(1)($\times 2$)=1.9949(8) and Mo-O(2)($\times 4$)=1.966(6)]. In ideal octahedral geometry Mo^{5+} has the triply degenerate electronic ground state $t_{2g}^1 e_g^0$ which is susceptible to a Jahn-Teller distortion as observed for NaTiO_2 .¹⁴ Orbital order resulting from a Jahn-Teller instability is a common origin for a distortion of octahedral coordination. The tetragonal compression of the MoO_6 octahedra below 353 K combined with the negative thermal expansion of the c lat-

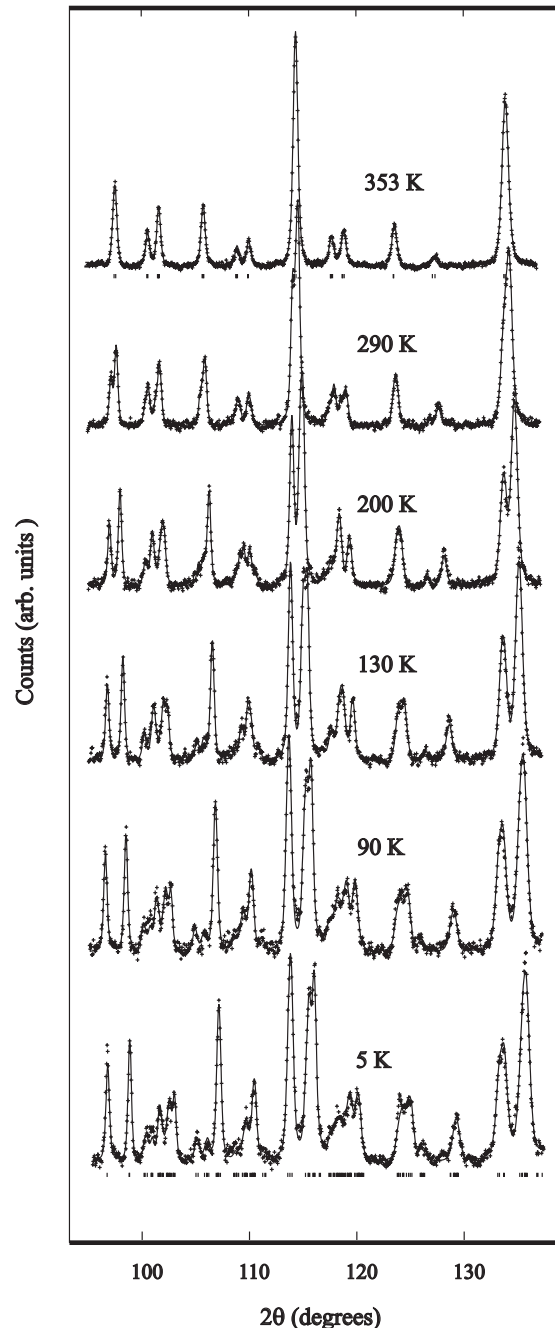


FIG. 2. A portion of the neutron-diffraction pattern of $\text{Ba}_2^{154}\text{SmMoO}_6$ evidencing two structural distortions below 353 and 130 K.

tice parameter (Fig. 4) suggests that partial orbital ordering may be responsible for the reduction in symmetry¹⁵ since the site symmetry of Mo in the triclinic structure, i , eliminates the double degeneracy of d_{xz} and d_{yz} observed in the tetragonal model. Similar partial orbital ordering has previously been evidenced from neutron powder-diffraction data of $\text{La}_{1+x}\text{Ca}_{1-x}\text{CoRuO}_6$ double perovskites.¹⁶

At 130 K, which corresponds to the antiferromagnetic transition temperature, a further distortion of the crystal structure is observed (Fig. 2). The MoO_6 octahedra distort so that there are two long bonds and four short bonds (Fig. 5)

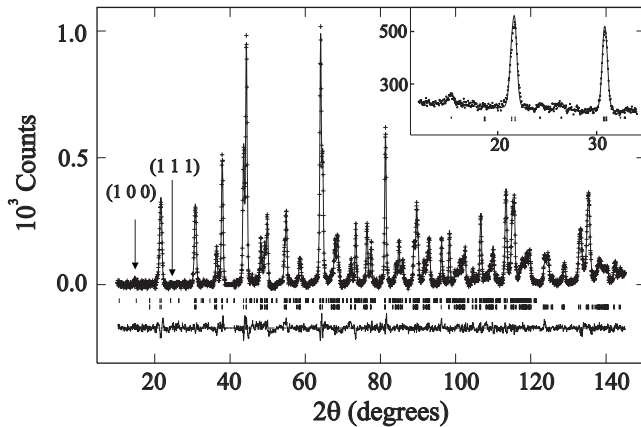


FIG. 3. Rietveld refinement fit to the 90 K neutron-diffraction pattern of $\text{Ba}_2^{154}\text{SmMoO}_6$. Data are excluded in the 2θ range of 39° – 41° due to a peak from the cryostat. The (100) and (111) magnetic Bragg reflections are indicated by an arrow. Top and bottom reflection markers correspond to magnetic and structural phases, respectively. The inset shows the low angle region showing the magnetic peaks which appear below T_N .

which result in tetragonal elongation of the MoO_6 octahedra. A Jahn-Teller distortion of the same magnitude is observed in NaTiO_2 (Ref. 14) which has the same ground-state electronic configuration. The observation of a Jahn-Teller distortion in transition-metal oxides with only t_{2g} electrons is rare as the Jahn-Teller interaction is much weaker than in manganese or copper oxides with partially filled e_g orbitals. Hence Jahn-Teller distortion of the octahedra is observed at much lower temperatures, e.g., a Jahn-Teller distortion of the TiO_6 octahedra is observed at 250 K in NaTiO_2 (Ref. 14) and at 130 K in $\text{Ba}_2^{154}\text{SmMoO}_6$. The observed tetragonal elongation of the MoO_6 octahedra suggests that the d_{xy} orbital is completely depopulated below 130 K. It is anticipated that the separation between d_{xz} and d_{yz} orbitals will be small so that the single electron in Mo^{5+} will occupy both orbitals, resulting in an elongation of the apical Mo-O(1) bond length. This distortion of the MoO_6 octahedra is manifest in the cell

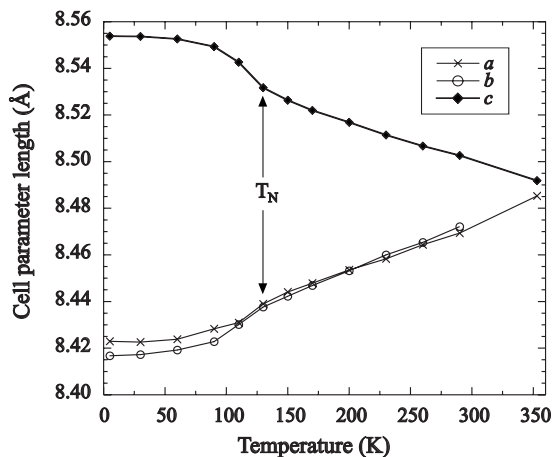


FIG. 4. The temperature variation in cell parameters for $\text{Ba}_2^{154}\text{SmMoO}_6$ evidencing a structural distortion at 130 K; a and b are multiplied by $\sqrt{2}$ for ease of comparison.

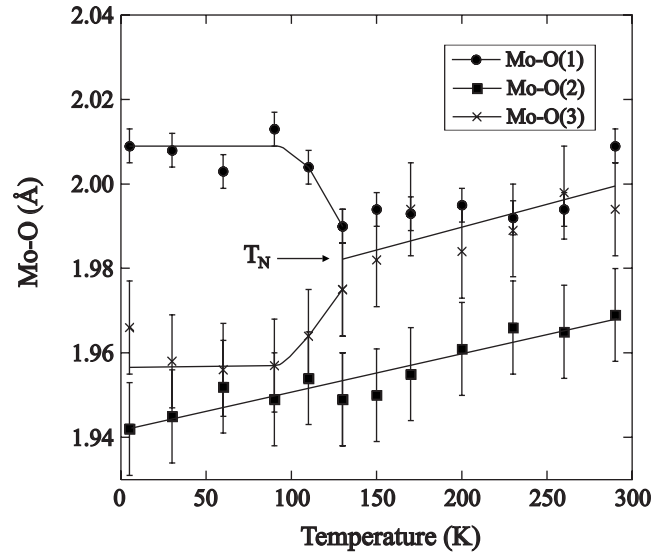


FIG. 5. Variation in Mo-O bond lengths with temperature evidencing a Jahn-Teller distortion at 130 K.

parameters which exhibit discontinuities at T_N (Fig. 4). Below T_N the reduction in b is greater than that in a as the Mo-O(3) bond is reduced to the same magnitude as the Mo-O(2) bond length. The variation in Sm-O bond lengths with temperature is displayed in Table I. The Sm-O(3) bond length increases near linearly (within error) with decreasing temperature and there is no anomaly at T_N which confirms that the larger reduction in b than a is as a result of the distortion of the MoO_6 octahedra at T_N .

Below 130 K antiferromagnetic order is evidenced in the neutron-diffraction patterns by the observation of weak antiferromagnetic (100) and (111) Bragg peaks (Fig. 3). These peaks are systematically absent from the triclinic $I-1$ structural model and can be indexed by a magnetic model with a primitive cell of the same dimensions as the I -centered nuclear cell. The best fit was obtained with a model containing two Mo^{5+} ions in the unit cell which were constrained to align antiparallel to one another. The magnetic spin was found to be ordered along either the x or y directions of the unit cell and the refined magnetic moment was $0.8(1)\mu_B$, which is close to the theoretical value of $1\mu_B$ expected for Mo^{5+} ions. It was not possible to determine if there was any magnetic order of the Sm^{3+} spins from the current data. The $^{154}\text{Sm}_2\text{O}_3$ isotope has a moderate absorption cross section for neutrons which resulted in a high background so that further data on a higher intensity instrument will be essential to solve the magnetic structure definitively.

Previous studies of antiferromagnetic order in Ba_2REMO_6 ($M=\text{Ru}, \text{Re}$) (Refs. 16 and 17) have demonstrated that T_N decreases as the rare-earth radius is reduced; T_N decreases from 100 K for $\text{Ba}_2\text{NdReO}_6$ to 33 K for $\text{Ba}_2\text{LuReO}_6$ (Ref. 17) (T_N of $\text{Ba}_2\text{SmReO}_6=82$ K). This occurs due to competition between M -O-RE and M -O-O- M exchange interactions; the former dominate for RE=Pr, Nd. The same pattern is not observed for the Ba_2REMO_6 double perovskites in which the Néel temperature, T_N , for $\text{Ba}_2\text{SmMoO}_6$ and $\text{Ba}_2\text{EuMoO}_6$ is almost an order of magnitude greater than that observed for $\text{Ba}_2\text{NdMoO}_6$ ($T_N=15$ K) in which super-

TABLE I. Fit parameters and refined Sm-O bond lengths between 4 and 290 K for Ba₂¹⁵⁴SmMoO₆.

Temperature (K)	χ^2	R_{WP} (%)	R_P (%)	Sm-O(1) ($\times 2$) (Å)	Sm-O(2) ($\times 2$) (Å)	Sm-O(3) ($\times 2$) (Å)
5	3.80	4.63	3.82	2.269(4)	2.278(12)	2.300(12)
30	3.78	4.52	3.81	2.270(4)	2.278(12)	2.303(12)
60	3.78	4.53	3.79	2.276(4)	2.299(12)	2.280(12)
90	3.76	4.55	3.75	2.262(4)	2.306(12)	2.278(12)
110	3.74	4.52	3.78	2.271(4)	2.310(12)	2.258(12)
130	3.82	4.64	3.86	2.280(4)	2.311(12)	2.259(12)
150	3.90	4.95	3.97	2.270(4)	2.309(12)	2.255(12)
170	3.81	4.66	3.78	2.268(4)	2.300(12)	2.247(12)
200	3.70	4.46	3.68	2.264(4)	2.299(12)	2.257(12)
230	3.81	4.63	3.79	2.269(4)	2.281(12)	2.263(12)
260	3.85	4.76	3.88	2.261(4)	2.282(12)	2.256(12)
290	3.86	4.78	3.88	2.252(4)	2.269(12)	2.267(12)
353	2.25	3.27	2.46	2.264(2)	2.299(8)	

exchange occurs via the Mo-O-Nd pathway so that the magnetic structure contains chains of ferromagnetically coupled Nd³⁺ and Mo⁵⁺ along the z direction aligned antiparallel to neighboring chains.⁷ As described above the magnetic diffraction peaks observed in the neutron-diffraction data below 130 K can be fit to a model containing two Mo⁵⁺ in the unit cell which align antiparallel to one another. This implies that the transition at 130 K is a result of superexchange via Mo-O-O-Mo as there is no evidence of magnetic ordering of the Sm³⁺ ion although further experiments are necessary to confirm this. There is no evidence of a Jahn-Teller distortion in the double perovskites Ba₂REMO₆ (M =Ru, Re) (Ref. 17) in which the highest T_N is observed for RE=Pr, Nd and hence it appears that the Jahn-Teller distortion (orbital order) observed at T_N in Ba₂¹⁵⁴SmMoO₆ enhances the superexchange between Mo nearest neighbors resulting in an anomalously high T_N =130 K, although further experiments are necessary to confirm the proposed superexchange pathways. There is no evidence of magnetic order for Ba₂RMoO₆ (R =Gd-Yb, Y); the Mo-O-O-Mo interaction will dominate in these materials⁷ which crystallize in the cubic $Fm\bar{3}m$ space group resulting in perfect magnetic frustration between Mo⁵⁺

spins which inhibits the formation of a magnetically ordered phase.

In conclusion, the results clearly demonstrate a strong interplay between spin, orbital, and lattice degrees of freedom in the $4d^1$ Mo⁵⁺ material Ba₂¹⁵⁴SmMoO₆ which gives rise to both structural and magnetic transitions with decreasing temperature. In Ba₂¹⁵⁴SmMoO₆ the orbital order is accompanied by an antiferromagnetic transition with an anomalously high T_N =130 K. It is anticipated that the high T_N observed in Ba₂EuMoO₆ also arises due to interactions between the spin and orbit degrees of freedom. Finally the results demonstrate that orbital degeneracy plays an extremely important role in molybdenum perovskites in determining the magnetic properties and that the synthesis of new Mo⁵⁺ oxides with the same spin orbital and lattice coupling could result in the observation of exotic magnetic and electronic properties.

ACKNOWLEDGMENTS

I thank the Leverhulme Trust for financial support, EPSRC-GB for provision of beamtime at the ILL, and A. Hewat and C. Ritter for assistance with the neutron experiments.

*Corresponding author; a.c.mclaughlin@abdn.ac.uk

¹C. N. R. Rao *et al.*, *Colossal Magnetoresistance, Charge Ordering and Related Properties of Manganese Oxides*, edited by C. N. R. Rao and B. Raveau (World Scientific, Singapore, 1998).

²H. D. Zhou *et al.*, *Phys. Rev. Lett.* **99**, 136403 (2007).

³S. Margadonna and G. Karotsis, *J. Am. Chem. Soc.* **128**, 16436 (2006).

⁴A. S. Erickson *et al.*, *Phys. Rev. Lett.* **99**, 016404 (2007).

⁵A. C. Mclaughlin, *Solid State Commun.* **137**, 354 (2006).

⁶C. D. Brandle and H. Steinfink, *Inorg. Chem.* **5**, 22 (1971).

⁷E. J. Cussen *et al.*, *Chem. Mater.* **18**, 2855 (2006).

⁸A. C. Mclaughlin (unpublished).

⁹E. J. Cussen, *J. Solid State Chem.* **180**, 474 (2007).

¹⁰H. M. Rietveld, *Acta Crystallogr.* **22**, 151 (1967).

¹¹A. C. Larson and R. B. Von Dreele, Los Alamos National Laboratory Report No. LAUR-86748, 1994 (unpublished).

¹²C. J. Howard *et al.*, *Acta Crystallogr., Sect. B: Struct. Sci.* **59**, 463 (2003).

¹³See EPAPS Document No. E-PRBMDO-78-114833 for Rietveld refinement results from variable temperature neutron-diffraction data. For more information on EPAPS, see <http://www.aip.org/pubservs/epaps.html>.

¹⁴S. J. Clarke *et al.*, *Chem. Mater.* **10**, 372 (1998).

¹⁵Jan-Willem G. Bos, J. P. Attfield, T. S. Chan, R. S. Liu, and L. Y. Jang, *Phys. Rev. B* **72**, 014101 (2005).

¹⁶N. G. Parkinson *et al.*, *J. Mater. Chem.* **15**, 1375 (2005).

¹⁷Y. Sasaki *et al.*, *J. Mater. Chem.* **12**, 2361 (2002).